

***Simple FEMs aren't as good as we thought:
experiences developing EIDORS v3.3***

Adler, Andy and Borsic, Andrea and Polydorides,
Nick and Lionheart, William R.B.

2008

MIMS EPrint: **2008.64**

Manchester Institute for Mathematical Sciences
School of Mathematics

The University of Manchester

Reports available from: <http://eprints.maths.manchester.ac.uk/>

And by contacting: The MIMS Secretary
School of Mathematics
The University of Manchester
Manchester, M13 9PL, UK

ISSN 1749-9097

Simple FEMs aren't as good as we thought: experiences developing EIDORS v3.3

Andy Adler¹, Andrea Borsic², Nick Polydorides³, William R B Lionheart⁴

Abstract – In this paper, we 1: announce EIDORS version 3.3, and clarify the new features and changes to the software. Briefly, the new version includes: a) interfaces to FEM generation (distmesh, netgen) and dual model solvers, b) new algorithms (total variation, electrode movement solver, temporal solvers), c) a data repository with *in vivo* and simulated data and models, d) faster algorithms with better caching, and e) improved graphics and extensive tutorials. 2: we review the use of dual models in EIT, and the architecture to support their use in EIDORS. 3: we discuss accuracy limitations to the single-order tetrahedral finite element models that are used in much EIT research. We recommend that models be used of at least 10^4 elements (for 2D FEMs) and 10^6 elements (for 3D FEMs). FEM accuracy may be partially addressed using dual model solvers, for which EIDORS v3.3 provides support.

¹Systems and Computer Engineering, Carleton University, Ottawa, Canada ²Thayer School of Engineering, Dartmouth College, Hannover, NH, USA ³School of Engineering, Massachusetts Institute of Technology, Boston, USA ⁴School of Mathematics, University of Manchester, UK

1 Introduction

We address three issues in this paper. First, we announce release version 3.3 of EIDORS (Electrical Impedance Tomography and Diffuse Optical Tomography Reconstruction Software), and report on the new features and their use. One significant addition is a repository for contributed experimental (physiological and phantom) and clinical data and FEM models, which we document here.

Next, we review the formulation of image reconstruction based on dual models, in which a refined fine FEM (finite element model) is used for the forward model, and a coarse mesh (not necessarily based on FEM) is used of image reconstruction. Dual models have been used in many EIT algorithms; we review their use, and provide an algorithmic framework to describe their application. EIDORS v3.3 provides an architecture to support general variations of dual models, which we describe.

Third, since dual models are designed to allow use of large FEMs for forward modelling, we explore the accuracy of the first order tetrahedral models that are most commonly used in EIT research. We report our experience that simple (tetrahedral first-order) finite element

models (FEMs) aren't as good as is generally assumed in EIT research. Our tests show that models with less than 2,500 elements (2D) and 150,000 elements (3D) are not able to reproduce the accuracy of tank phantom measurements. This effect is particularly severe in 3D FEM models, because the number of elements required to achieve a given element minimum dimension is larger by a power of $\frac{3}{2}$.

2 EIDORS version 3.3

EIDORS (Electrical Impedance Tomography and Diffuse Optical Tomography Reconstruction Software) is an open source suite of software for reconstruction of images in soft field tomography modalities. The earliest version[5] was made available in 1999 and provided support for 2D EIT (documented in [9]). Subsequently, support for 3D EIT was provided[7] in 2002. In 2005, a software refactoring was performed on the EIDORS software base to allow “pluggability” – easy incorporation of contributed algorithms and functionality – as part of EIDORS version 3 (while the previous releases were renamed v1 and v2, respectively). This provides many of the key features of object oriented software, which helps to structure such large software projects. Version 3.0 was released in 2005[2], v3.1 in 2006 (and described in [1]), v3.2 in 2007, and v3.3 (described in this paper). Many new features have been added; in terms of lines of code, v2.0 has 3715, v3.0 has 10685 and v3.3 has 22424 (with another 11705 in tutorials).

The following high-level new features are part of EIDORS v3.3:

2.1 Interfaces to FEM generation tools: (Netgen[8] and Distmesh[6])

2.2 Support for dual model solvers:

2.3 New reconstruction algorithms: total variation, electrode movement solver, temporal solvers

2.4 Data repository: with several contributed models, clinical and experimental data sets

2.5 Faster algorithms: for calculation of Total Variation PDIPM, Jacobian; better caching; an iterative forward solver (to save memory, if required)

2.6 Improved graphics and extensive tutorials

3 Data Repository

EIDORS incorporates a data repository which includes animal and clinical experimental EIT data (including the earliest EIT measurements[3]), calibrated phantom data, and FEM models and simulation data. The goal of the EIDORS data repository is to: 1) allow new researchers in the community to have some real data against which they can test their software, and 2) allow testing of algorithms against available and standard benchmark data.

Licensing of contributed data depends on the choice of the owners of each contribution. The default license is the Creative Commons Artistic License (with attribution). This license allows copying, distribution, and derivative works with the requirement that the user give the author credit as specified. Generally, contributed data forms part of a published study, and the credit requirement is fulfilled by referencing the original study.

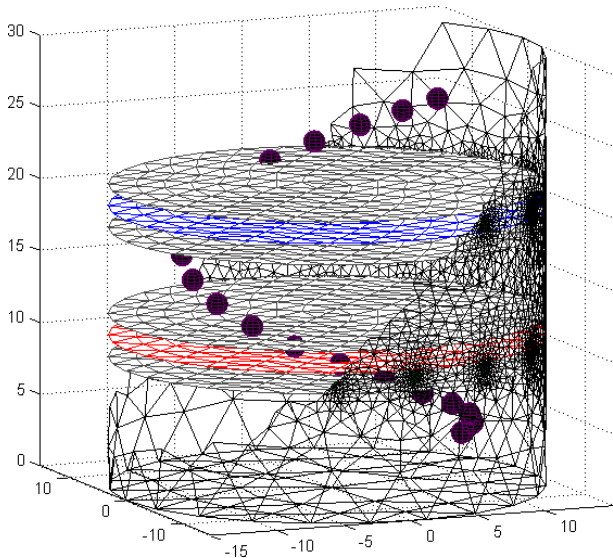


Figure 1: Netgen model of a 2×16 electrode tank. The positions of the simulated conductive target moving in a helical path are shown in purple. The 3D fine model is shown (cropped). The upper (blue) and lower (red) layers corresponding to the geometry of the coarse model are shown. The z -direction limits of the coarse model are shown in grey.

4 Dual Model solvers

A dual reconstruction model uses a high density (fine) FEM to implement the forward solution (voltages at electrodes), and a low density (coarse) mesh (not necessarily FEM based) for the inverse solution. For example, a dual model may be used to represent the conductivity change in a layer of a 3D plane (Fig. 1). Given a forward model, F , which calculates a voltage measurement vector, \mathbf{v} , from a forward (fine) model conductivity element vector, $\boldsymbol{\sigma}_f$, we have $\mathbf{v} = F(\boldsymbol{\sigma}_f)$. The reconstruction (coarse) model is defined on square elements $\boldsymbol{\sigma}_r$, related by a coarse to fine projection matrix \mathbf{P} , where $\boldsymbol{\sigma}_f = \mathbf{P}\boldsymbol{\sigma}_r$.

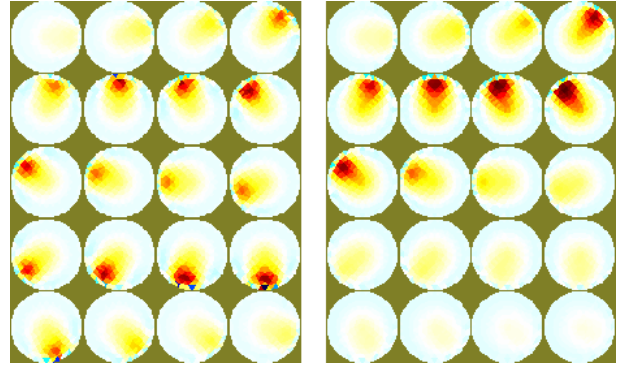


Figure 2: Reconstructed images of a target moving in a helical pattern using difference reconstruction models. *Left* reconstruction model with $z_{depth} = \infty$ *Right* reconstruction model with $z_{depth} = 0.1 \times \text{scale}$ at lower position in Fig. 1

This is implemented in EIDORS as follows. For each inverse model, represented as part of the `inv_model` structure (Fig. 3), there are two `fwd_model` structures: 1) the refined forward model `fwd_model`, and 2) the reconstruction model `rec_model`. Within each forward model structure is a matrix field `coarse2fine` which is a sparse encoding of \mathbf{P} . Each element $[\mathbf{P}]_{i,j}$ represents the fraction of fine element i enclosed within coarse element j .

The Jacobian matrix may be defined for the coarse (\mathbf{J}_r) and fine (\mathbf{J}_f) models as follows:

$$\mathbf{v} = \mathbf{J}_f \boldsymbol{\sigma}_f = \mathbf{J}_f \mathbf{P} \boldsymbol{\sigma}_r = \mathbf{J}_r \boldsymbol{\sigma}_r \quad (1)$$

and thus $\mathbf{J}_r = \mathbf{J}_f \mathbf{P}$. Since the matrix \mathbf{J}_f is very large, EIDORS will not calculate it directly. Instead, an efficient algorithm calculates each column of \mathbf{J}_r using

$$[\mathbf{J}_c]_{i,j} = [\mathbf{J}_f \mathbf{P}]_{i,j} = \sum_k \frac{\partial[\mathbf{v}]_i}{\partial[\boldsymbol{\sigma}_f]_k} [\mathbf{P}]_{k,j} = \frac{\partial[\mathbf{v}]_i}{\partial[\boldsymbol{\sigma}_c]_j} \quad (2)$$

where the last expression is implemented in terms of the FEM system matrix using the adjoint field method.

The need for a matrix \mathbf{P} on the `rec_model` is due to the limits of the first order FEM representation. If the regions in the reconstruction model are not triangular, then each region is constructed from triangular regions and the parametrization represented in \mathbf{P} .

Dual meshes may be used in several applications:

- o Corresponding meshes: where coarse elements completely contain fine ones but do not cross elements.
- o Nodal Solvers: in which the reconstruction parameterizes the conductivity on each node[4].
- o $2\frac{1}{2}$ D Solvers: in which the z -dimension of the 3D fine model is projected onto a 2D reconstruction model. This technique is widely used in geophysical applications.
- o Constraining Reconstruction Parameters: this is useful for example to have one parameter for out of plane conductivity (a region of low sensitivity), which may prevent the algorithm from “pushing” artefacts there.

```

inv_model
├── name:          'text string of model name'
├── type:          'inv_model'
├── solve:         eg. np_inv_solve
├── RtR_prior:    eg. laplace_image_prior
├── R_prior:      } provided if no RtR_prior
├── hyperparameter
│   ├── value:    eg. 1e-8
│   ├── func:     eg. aa_calc_noise_figure } optional
│   └── parameters: eg. noise_figure
├── jacobian_bkgnd
│   ├── value:    eg. 1
│   └── func:     fcn to estimate bkgnd } optional
├── meas_icov:    fcn to calc (noise cov)-1 } optional
├── reconst_type: eg. difference
├── fwd_model:    fine model (fwd model)
└── rec_model:    reconst model (fwd model)} optional

```

Figure 3: Layout of the EIDORS `inv_model` object

- o Solving to a Square Pixel Grid: this is useful because the reconstructed image is typically mapped to pixels, and will often show artefacts based on the shapes of the elements. A rasterized reconstruction grid will prevent such artefacts, and allow more natural communication of the underlying system resolution (via the pixel size).

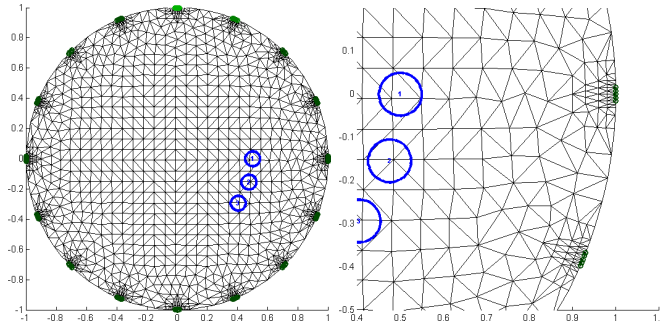


Figure 4: Simulation FEM and simulated target positions in blue *Left* full scale mesh. *Right* mesh magnified near target positions

5 FEM accuracy

Finite Element Model accuracy is normally considered from the point of view of voltage errors between FEM and physical phantom. While this is correct, any errors may be explained by small details in the phantom which are not considered in the model. This means that it is difficult to use such a test to verify high model accuracy, which is necessary in a soft field tomography modality. Instead, we consider FEM accuracy by looking at small changes in the model and the consequences on difference EIT images.

The easiest (and most common) way to simulate a moving target in a medium is to use a single FEM to select and then interpolate which elements are part of that target. There is no change to the underlying FEM, and thus no model noise in the images.

To illustrate this process, Fig. 4 shows two 2372 element

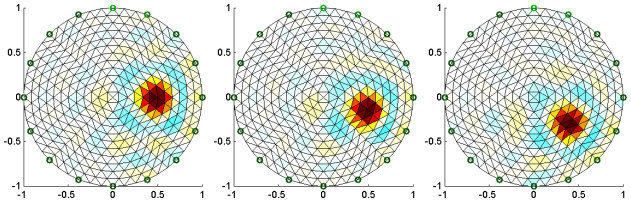


Figure 5: Images reconstructed from simulations interpolating shapes in Fig. 4; from left to right, targets 1 to 3. No model noise is seen in the images.

FEMs created by `distmesh`, with mesh refinement near the electrodes. Electrodes are simulated using a Sheffield-type adjacent stimulation and measurement. For each simulated target position (blue), the fraction of each element filled by the target is calculated and used to scale the simulated conductivity change in the element. Images are reconstructed of the three target positions in Fig. 5 using a one-step regularized GN image reconstruction. No noise is seen from the simulation, as expected, since the FEM model does not change.

However, the most appropriate way to simulate a moving target is create a target region within the FEM and to remesh around it. This means that the mesh changes between each target position, not only near the target, but throughout the FEM due to the propagation of changes in triangularization.

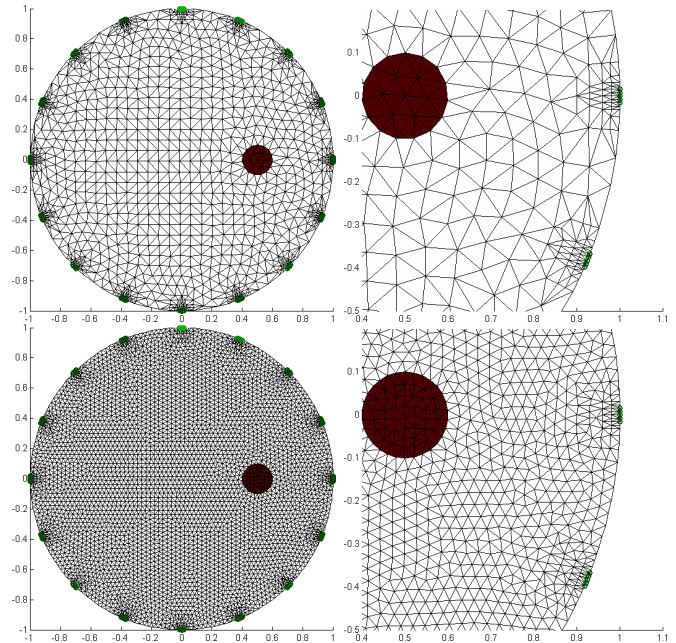


Figure 6: Simulation FEM and simulated target positions in blue *Left* full scale mesh. *Right* mesh magnified near target positions *Top* FEM with 2372 elements, *Bottom* FEM with 8909 elements,

Using `distmesh`[6], FEMs were created of a homogeneous phantom (like that of Fig. 4), and of three phantoms with inset targets areas in the corresponding positions. Fig. 6 shows the mesh at the first target position.

Three different levels of mesh refinement are shown.

Based on these simulations, we reconstruct images using a simple 576 element reconstruction model with point electrodes (Fig. 7). In the coarse (2372 element) and to a lesser extent in the refined (8909 element) mesh, there are artefacts, mostly near the electrodes, which dramatically disturb the image clarity.

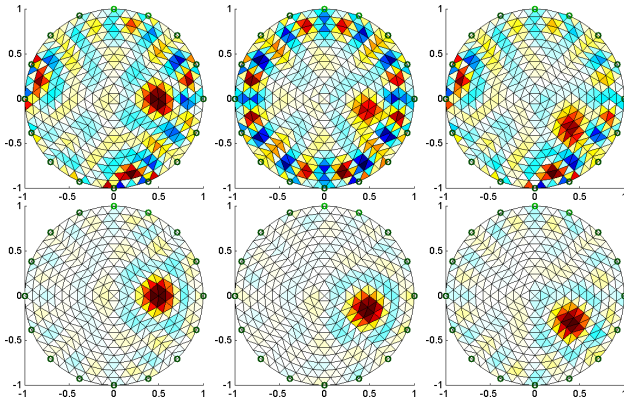


Figure 7: Images reconstructed of targets simulated from interpolated shapes in Fig. 6, from left to right, targets 1 to 3. *Top* FEM with 2372 elements, *Bottom* FEM with 8909 elements,

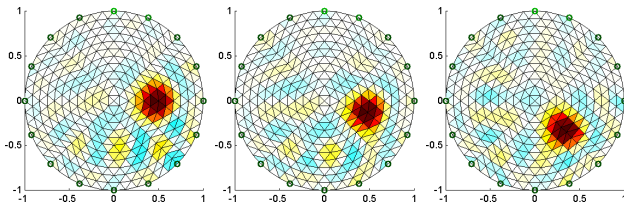


Figure 8: Images reconstructed of a target in a saline tank with the same reconstruction parameters as Fig. 7.

To compare with these images, a sequence of EIT data were gathered with a 16 electrode system from the IIRC from Kyung Hee University, Korea. A saline filled tank was used and a small non-conductive target was slowly rotated around the tank. Frames of data corresponding to the simulated positions are shown. Images are reconstructed from these data using the same reconstruction parameters and shown in Fig. 8. These images show some artefacts in the lower part of the image (probably due to waves in the tank from the movement), but show less of the artefacts (near the electrodes) seen in Fig. 7.

The same effect can be seen in 3D FEM, and is even more significant because the number of elements required to achieve a minimum element dimension is larger in 3D by approximately a power of $\frac{3}{2}$. Fig. 9 shows an example of a ball of the same radius as the 2D examples introduced into a 131,640 element FEM using netgen[8]. Significant artefacts are seen, even for a very large model size. We have currently not been able to generate sufficiently large FEM models to eliminate reconstruction artefacts, due to memory constraints on our systems.

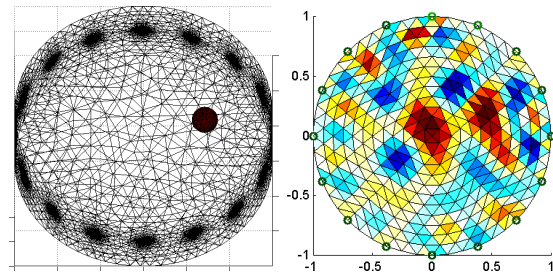


Figure 9: *Right*: 3D models from netgen [8] of a moving ball in a 16 electrode tank with 131,640 elements. *Left*: Image reconstructed using the same parameters in the previous figures. Significant artefacts are shown, due to the inadequate element size.

6 Discussion

In this paper we: 1) announce EIDORS version 3.3, and clarify the new features and changes to the software; 2) review the use of dual models in EIT, and the architecture to support their use in EIDORS; and 3) discuss the accuracy limitations to the single-order tetrahedral finite element models that are used in much EIT research. As a preliminary recommendation, we suggest a minimum model size of 10^4 elements (2D FEM) and 10^6 (3D FEM).

References

- [1] Adler A and Lionheart WRB (2006) Uses and abuses of EIDORS: An extensible software base for EIT. *Physiol. Meas.* 27:S25–S42
- [2] Adler A and Lionheart WRB (2005) EIDORS: Towards a community-based extensible software base for EIT *Conf. Biomedical Applications of EIT* London, UK, June 22-24
- [3] Barber BC Brown BH and Freeston IL, (1983) Imaging spatial distributions of resistivity using applied potential tomography, *Electronics Lett*, 19:933–935
- [4] Graham B and Adler A, (2006) A Nodal Jacobian Algorithm for Reduced Complexity EIT Reconstructions *Int. J. Inform. Systems Sciences*, 2:453–468.
- [5] Lionheart WRB, Arridge SR, Schweiger M, Vauhkonen M and Kaipio JP (1999) Electrical Impedance and Diffuse Optical Tomography Reconstruction Software *World Congress Indust. Proc. Tomog.*, Manchester, UK, April 14-17
- [6] Persson P-O and Strang G (2004) A Simple Mesh Generator in MATLAB *SIAM Review* 46:329–345
- [7] Polydorides N and Lionheart WRB (2002) A Matlab toolkit for three-dimensional electrical impedance tomography: a contribution to the Electrical Impedance and Diffuse Optical Reconstruction Software project *Meas. Sci. Technol.* 13:1871–1883
- [8] Schöberl J (1997) NETGEN: An advancing front 2D/3D-mesh generator based on abstract rules *Comput. Visual. Science* 1:41–52
- [9] Vauhkonen M, Lionheart WRB, Heikkinen LM, Vauhkonen PJ and Kaipio JP (2001) A MATLAB package for the EIDORS project to reconstruct two-dimensional EIT images *Physiol Meas* 22 107-111